

Conformational Studies of the 313-320 and 313-332 Peptide Fragments Derived from the α_{IIb} Subunit of Integrin Receptor with Molecular Dynamics Simulations

Athanassios Stavrakoudis

Accepted: 9 July 2009 / Published online: 24 July 2009
© Springer Science+Business Media, LLC 2009

Abstract The peptide sequence YMESRADRKLAEVG-RVYLFL, derived from 313-332 region of the α_{IIb} , has been identified as a potent inhibitor of platelet aggregation and fibrinogen binding to $\alpha_{IIb}\beta_3$. More detailed studies have revealed that the $Y_{313}MESRADR_{320}$ sequence is the shortest octapeptide with strong inhibitory activity. This work provides insight of the solution conformation of these peptides, by performing extensive molecular dynamics simulations of 100 ns. The 8mer peptide has no stable conformation in water while the 20mer peptide retains a relative conformational stability. Analysis of side chain orientation of the RAD fragment revealed the synplanar arrangement of guanidinium and β -carboxylic groups providing a framework for explaining the similar biological activity of the two peptides, despite their differences in sequence and conformation.

Keywords Computer simulation · Integrin · Molecular dynamics · Peptide conformation · Platelet aggregation inhibition · SAR · α_{IIb}

Introduction

Integrins are receptors that mediate many biological important processes (Humphries 2000). They are heterodimers which come into non-covalent association and they are composed by two membrane proteins. The integrin $\alpha_{IIb}\beta_3$ (glycoprotein IIb/IIIa) has a very significant role in thrombosis and haemostasis. It mediates interactions between

platelets and several ligands, primarily fibrinogen (Phillips et al. 1988). Integrins are well known for their recognition of protein ligands through the RGD sequence (Salsmann et al. 2006; Takada et al. 2007). Crystallization of integrin segments with RGD ligands has revealed important features of the binding mode (Xiao et al. 2004; Xiong et al. 2002), such as binding to the α subunit β propeller exposed interface. One Mg^{2+} ion participates in integrin binding of RGD peptides (Craig et al. 2004; Xiao et al. 2004) by coordinating to the Asp side chain, while guanidinium group of Arg side chain binds to carboxylic side chains of Asp residues located at the α subunit β propeller domain (Xiong et al. 2002).

Recently, the sequence of the α_{IIb} subunit has been mapped with 20mer peptides for identifying fibrinogen binding domains (Biris et al. 2003a). The most promising region, thus the 313-332 fragment, was further investigated (Mitsios et al. 2004, 2006), in order to define important residues for its activity and minimum chain length that can retain the inhibitory and aggregatory capability. These investigations revealed that the peptide sequence $Y_{313}MESRADR_{320}$, located at amino terminus of the initial 20mer, is a putative fibrinogen-binding region by inhibiting platelet aggregation and by antagonizing fibrinogen association (Mitsios et al. 2004). Biological activity of the peptide was attributed primarily to the (highly conserved in the integrins) RADR motif (Mitsios et al. 2006; Stanica et al. 2008). Interestingly it was found that the peptide lost its inhibitory activity after deletion of the amino terminus YMES sequence, indicating that the carboxyl terminus RADR motif is not capable to act independently from the rest of sequence, despite its similarity with the well known RGD motif. On the other hand, alanine scanning of the $Y_{313}MESRADR_{320}$ sequence revealed that substitution of each of the Y_{313} , M_{314} , E_{315} or S_{316} residues does not affect biological activity (Stanica et al. 2008). Inhibitory activity

A. Stavrakoudis (✉)
Department of Economics, University of Ioannina,
45110 Ioannina, Greece
e-mail: astavrak@cc.uoi.gr
URL: <http://stavrakoudis.econ.uoi.gr/>

has also diminished after elongation of the Y_{313} MES-RADR₃₂₀ sequence from both amino and carboxyl terminus. Since there is no structural information for the peptide, these observations were ascribed to the strand conformation of the residues surrounding the RADR fragment, as found in the crystal structure integrin/fibrinogen complex (Xiao et al. 2004).

This work presents a computer simulation study of the aqueous conformation of the Y_{313} MESRADRKLAEVGRVYLFL₃₃₂ and Y_{313} MESRADR₃₂₀ peptide sequences derived from the α_{IIb} integrin subunit. State of art molecular dynamics protocols have been applied in order to elucidate the most important characteristics of their conformational and dynamical properties. Molecular dynamics simulations offer a solid background for studying biomolecular structure and interactions. This computational based approach has been shown to be very valuable and its importance is well described (Hansson et al. 2002; Karplus and McCammon 2002; Morikis and Lambris 2004; van Gunsteren and Berendsen 1990; van Gunsteren et al. 2008). Similar computational approaches have been showed to add valuable information to existed experimental data of antibody/antigen complexes (Lorenzo et al. 2007; Tatsis et al. 2009b; Voordijk et al. 2000), to explore the dynamics of peptide/MHC interactions (Painter et al. 2008; Wan et al. 2004; Yaneva et al. 2009; Zacharias and Springer 2004), in searching for active conformational templates (Stavrakoudis et al. 1997, 2003; Tatsis et al. 2006, 2008), to establish a model of protein/peptide dimerization based on a disulfide bridge (Stavrakoudis 2009b), to analyze hydrophobic clusters of protein structures (Espinoza-Fonseca 2009; Tatsis et al. 2009), to analyze the non-bonded interactions that stabilize secondary structures in peptides (Santiveri et al. 2004; Stavrakoudis et al. 2009; Wang and Sung 1999; Yoda et al. 2007), or to explore pathways of protein folding (Duan and Kollman 1998; Karplus and Sali 1995; Morra et al. 2008). Atomistic simulations of peptides provide an excellent framework to study the intrinsic flexibility of peptides and to describe the non-bonded interactions that contribute to peptide's structure and/or function, something that is not always accessible with other experimental methods (Hansson et al. 2002; van Gunsteren and Berendsen 1990; Voordijk et al. 2000).

Methods

Molecular mechanics and/or dynamics simulations were performed with NAMD (Phillips et al. 2005). The coordinates of the initial structure of Y_{313} MESRADR₃₂₀ (from this point on P1 or 8p) and Y_{313} MESRADRKLAEVGRVYLFL₃₃₂ (from this point on P2 or 20p) peptides were extracted from PDB's (Berman et al. 2000) entry 1txv (Xiao

et al. 2004). Hydrogen atoms were added with the autopsf utility of the VMD program (Humphrey et al. 1996). The peptides were solvated with TIP3P (Jorgensen et al. 1983) water molecules in an orthogonal parallelepipedon box, leaving a distance of at least 1.8 nm of any peptide atom to the edge of the solvent box. The final dimensions of the boxes were $4.98 \times 5.94 \times 4.65 \text{ nm}^3$ in the P1 case and $5.68 \times 7.46 \times 5.02 \text{ nm}^3$ in P2 case. Ten pairs of Na^+ and Cl^- counter ions were added in the box containing the P1 peptide. Fourteen Na^+ and fifteen Cl^- ions were added in the P2 box. Both P1 and P2 systems were treated similarly from this point on. In the first step, energy minimization was performed for 2,500 steps under PBC conditions. The non-bonded pair list was updated every 10 steps, while non-bonded interactions were computed every second step. Long range electrostatics were computed with the PME method (Darden et al. 1993; Toukmaji and Board 1996) every second step, with a grid spacing of less than 0.1 nm. Bonds to hydrogen atoms were constrained with the SHAKE (Barth et al. 1995; van Gunsteren and Berendsen 1990) algorithm, with a relative tolerance of 10^{-8} , allowing a 2 fs step during subsequent MD runs. Heavy atoms of the peptide were restrained to initial coordinates with a force constant of $50 \text{ kcal } \text{\AA}^{-1} \text{ mol}^{-2}$. After minimization, the temperature of the system was gradually increased with Langevin dynamics using the NVT ensemble to 310 K during a period 3,000 steps, by stepwise reassignment of velocities every 500 steps. Simulation was continued until 10^5 steps. After this point, the force constant of heavy atoms restraint were reduced to $5 \text{ kcal } \text{\AA}^{-1} \text{ mol}^{-2}$, and the simulation was continued for another 10^5 steps. Equilibration was finalized with 2×10^5 steps of Langevin dynamics under NVT conditions by totally eliminating the positional restraints. The simulation was continued under constant pressure, with Langevin piston method (Feller et al. 1995), thus NPT ensemble, for 100 ns (5×10^7 steps). Pressure was maintained at 1 atm and temperature was kept at 310 K. Structures were saved to disk every 500 steps (1 ps) for further analysis.

Conformational Analysis

Conformational analysis and visual inspection of structures were performed with VMD (Humphrey et al. 1996), Carma (Glykos 2006) and Eucb (Tsoulos and Stavrakoudis 2009) software packages. Appropriate circular statistics were taken into consideration for calculation of descriptive values of dihedral angles (Döker et al. 1999). Trajectory analysis of hydrogen bonds were performed with a single geometrical criterion: a hydrogen bond was accepted if the Acceptor–Donor distance was less than 0.33 nm and the Donor–Hydrogen–Acceptor angle greater than 120° . Hydrophobic interactions were assigned when two non-polar heavy atoms were in less than 0.4 nm distance

proximity. Secondary structure assignment was performed with STRIDE (Frishman and Argos 1995). Structural figures were prepared with PYMOL (Delano 2002).

The root mean square distance (RMSD) between the backbone atoms of the trajectory frames of polypeptide chains and the corresponding atoms of the X-ray structure, calculated for frame t , is given by Eq. 1, where x^m, y^m, z^m are the Cartesian coordinates found at the X-ray structure and x^t, y^t, z^t are the Cartesian coordinates of trajectory frame t . N is the number of atoms.

$$\text{RMSD}_t = \frac{1}{N} \sqrt{\sum_{i=1}^N (x_i^m - x_i^t)^2 + (y_i^m - y_i^t)^2 + (z_i^m - z_i^t)^2} \quad (1)$$

Secondary structure assignment of trajectory frames was performed with the STRIDE program (Frishman and Argos 1995). STRIDE assigns one letter code for each residue of a protein sequence, so E stands for strand conformation, T stands for turn, C stands for coil and B stands for bridge. Hydrogen bonds assignment was based on geometrical criteria: Donor–Acceptor distance less than 0.33 nm and Donor–Hydrogen–Acceptor angle greater than 120° . β -turns were defined by the $C^\alpha(i)–C^\alpha(i+3)$ distance to be less than 0.7 nm and the $C^\alpha(i)–C^\alpha(i+1)–C^\alpha(i+3)–C^\alpha(i+3)$ dihedral to be less than 90° (absolute value). Root mean square fluctuation deviation (RMSD) measurements were performed after the removal of the global translation/rotation of the trajectory frames. Structural figures were prepared with PYMOL (Delano 2002).

Conformational Clustering

Assignments of secondary structure of the peptide frames with the STRIDE program were stored into a database and conformations of the trajectories were clustered using simple SQL queries.

Entropy Calculations

Schlitter's formulation (Schlitter 1993) was used for the calculation of the configurational entropy (S):

$$S_{\text{true}} < S = \frac{1}{2} k_B \ln \det \left[1 + \frac{k_B T e^2}{\hbar^2} \mathbf{M} \boldsymbol{\sigma} \right] \quad (2)$$

where S is an upper estimation of the true entropy (S_{true}), k_B is Boltzmann's constant, T is the absolute temperature (in which the system was simulated), e is Euler's number, \hbar is Plank's constant divided by 2π , \mathbf{M} is the mass matrix that holds on the diagonal the masses belonging to the atomic Cartesian degrees of freedom, and $\boldsymbol{\sigma}$ is the covariance matrix of atom positional fluctuations:

$$\sigma_{ij} = (x_i - \langle x_i \rangle)(y_i - \langle y_i \rangle) \quad (3)$$

Entropy calculations were performed with the backbone atoms (N, C^α and C') of the peptide from the bound and free trajectories respectively, at 0.1 ns interval (100 frames).

Two separate trajectories (for example A and B) can be combined, thus one trajectory can be appended at the end of the other trajectory, and the plot of configurational entropy S against time can be used as assessment of the overlap between configurational spaces sampled in two simulations (Hsu et al. 2005). Such trajectories have been derived for the backbone (bb) atoms (N, C^α , C') of the peptide from the last 80 ns of the P1 (8mer) and P2 (20mer) trajectories, taking into consideration the common fragment 314–319. N- and C-terminal residues from the 8mer peptide were excluded from the analysis, due to their increased mobility. Similar analysis has been applied to reveal coverage of conformational space between free and bound trajectories on peptide/antibody binding study (Stavrakoudis 2009a). Both appending sequences were applied resulting in $S_{\text{bb}}^{\text{P1+P2}}$ and $S_{\text{bb}}^{\text{P2+P1}}$ calculations, where the P2 trajectory was appended to the P1 trajectory (P1 + P2) or the P1 trajectory was appended to the P2 one (P2 + P1). Plotting the calculated values of S from both the combined trajectories over time demonstrates the relative size and overlap of sampled trajectories. Plotting of S over time after the combination of two trajectories results in three cases (Hsu et al. 2005), briefly described as:

1. S increases after appending one trajectory after to the other, with a jump observed at this point, thus the two trajectories do not overlap, or there is only a small overlap between them.
2. S evolves smoothly after the appending of the trajectories, without an observable perturbation of the line of S over time, thus the two trajectories show significant overlap.
3. S curve increases during the time of the first trajectory but decreases a little after the appending of the second trajectory, thus the second trajectory samples a smaller configurational space than the first one, which also contains the configurational space visited by the second one.

Such an analysis of the combined trajectories is more advantageous than comparing directly the configurational entropies of two independent trajectories and can provide information about the extent of sampling overlap (if any) between two trajectories. The coverage of the P1 trajectory with respect to the P2 trajectory is:

$$\Delta S_{\text{bb}}^{\text{P2+P1}} \equiv S_{\text{bb}}(\text{P2}) - S_{\text{bb}}(\text{P1}) \quad (4)$$

and the coverage of the P2 trajectory with respect to the P1 trajectory is:

$$\Delta S_{\text{bb}}^{\text{P1+P2}} \equiv S_{\text{bb}}(\text{P1}) - S_{\text{bb}}(\text{P2}) \quad (5)$$

Results and Discussion

Crystal Structure Analysis

The structure of a_{IIb} is composed by beta propeller repeats and the 313–332 fragment is found at the surface of the structure (W5 blade of the a_{IIb} subunit) in an exposed region, connecting the β_2 and β_3 antiparallel β -strands (Xiao et al. 2004). The 313–332 fragment of a_{IIb} (α subunit) has a remarkable position on the crystal structure of integrin (Xiao et al. 2004), Fig. 1. Secondary structure of the 20mer peptide was found in TEEEETTTEEEECCEEEEEEC state, thus mainly in strand conformation. The fragments Met₃₁₄-Arg₃₁₇ and Lys₃₂₁-Glu₃₂₄ form two antiparallel β -strands that are connected with two consecutive type IV β -turns consisted by the Ala₃₁₇-Asp₃₂₀ and Asp₃₁₈-Arg₃₂₁ fragments. Backbone hydrogen bonds between Val₃₂₅:N-Tyr₃₁₃:O, Glu₃₁₅:N-Ala₃₂₃:O, Ala₃₂₃:N-Glu₃₁₅:O stabilize this β -hairpin conformation.

Convergence of Simulations

The need of good conformational sampling of biomolecular simulations is very well described in the literature (Smith et al. 2002). Here, two long (100 ns) molecular dynamics trajectories have been produced in order to ensure to that the peptides have visited different areas of the conformational space. Moreover, two more checks have been employed in order to estimate the goodness of the conformational sampling during simulation time.

First, cluster analysis (according to secondary structure assignment with STRIDE) revealed that, in the case of P2 (20mer) trajectory that 22 backbone conformations existed with population over 1%, during the whole simulation time of 100 ns. Splitting the trajectory into two equal

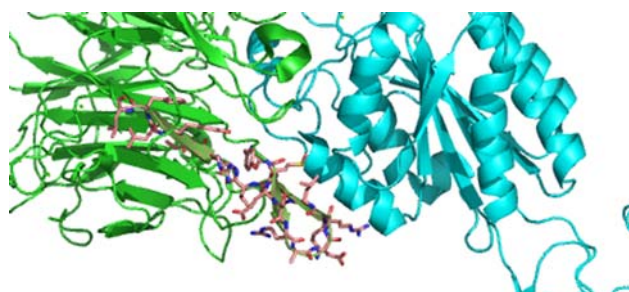


Fig. 1 Location of the 313–332 sequence of the a_{IIb} chain of the integrin receptor. PDB's entry 1txv was used. Protein is rendered with *ribbons* and the 313–332 sequence is shown with *sticks*

parts of 50 ns revealed that there were 23 different conformations in the first part and 21 in the second one (with population over 1%). The results were quite similar, when a 0.5% cutoff was applied: 43 conformations were found in the whole trajectory, while 47 and 45 different conformations were found in the first and second part of the P2 trajectory, respectively. These findings clearly indicate the convergence of the simulation. Similar results were obtained with the P1 (8mer) trajectory, although the second part of the P1 trajectory revealed a somewhat reduced number of conformations in comparison with the first one.

A second check of the simulation convergence was performed with entropic analysis of the backbone conformation of the fragment 314–319 of the P1 (8mer) peptide. N- and C-terminal residues were excluded from analysis due to their increased flexibility. The 100 ns trajectory was split in two parts of 50 ns and the last 30 ns were taken into consideration for entropy calculations, resulting in two (*A* and *B*) sub-trajectories. Only backbone atoms were included. Plotting the entropy curves of trajectories *A* + *B* (appending *B* to *A*) and *B* + *A* (appending *A* to *B*) is shown in Fig. 2. According to the analysis of Hsu et al. (2005), Figure 2 reveals the overlapping of the two parts of the initial trajectory, as the line of entropy (*S*) does not show a significant perturbation after the append of trajectory part to the other. This indicates the frame from two distinct parts of the trajectory visited similar conformations, thus the simulation resulted in good sampling of the conformational space. This is something to be expected, as the simulation time was above the usual applied 30–50 ns in peptide simulations (Smith et al. 2002) but this is always a hypothesis until tested with some of the methods proposed by Smith et al. (2002). Evidence provided here corroborate the assumption of conformational convergence and thus provide a solid background for further conformational analysis.

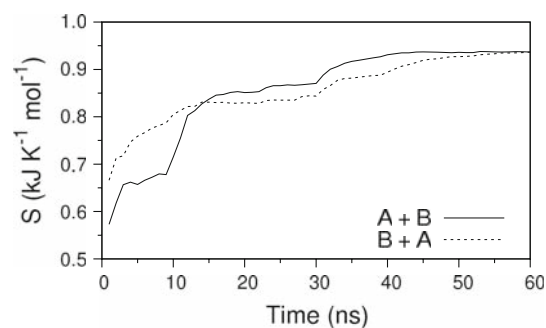


Fig. 2 Plot of estimated entropy of backbone atoms of the P1 peptide (fragment 314–319). The P1 trajectory was split in two parts (*A*, *B*) of 50 ns. The last 30 ns of each trajectory were appended to each other. See [Methods](#) for details of calculation

RMSD Analysis

RMSD time evolution of backbone atoms of peptides P1 and P2 is presented at Fig. 3. The initial X-ray structure was used as a reference. Here, it is interesting to see the RMSD value of the common fragment (314–319) of the two peptides. As it can be seen, both peptides experienced relatively large deviations from the initial structure with RMSD values in the range of 0.25–4.5 nm. Both peptides escaped from the crystal structure conformation during the equilibration period. Interestingly, the P2 peptide showed relatively lower RMSD values (0.2–0.3 nm) during a period of approximately 60 ns, from the 7th to 67th ns of the simulation time. During the same period the P1 peptide showed increased RMSD values with a peak of 0.45 nm at approximately 24 ns. After the 65th ns of the simulation both peptides showed RMSD fluctuations around 0.2 nm.

Examination of Fig. 3 reveals that the 314–319 fragment of the P2 peptide showed decreased mobility relative to the rest of the molecule and remained closer to the starting conformation of the crystal structure. It is evident also, that the conformation of the 8mer N-terminal part of the P2 peptide is different from the conformation of the P1 peptide which has the same sequence. The loss of the starting conformation of a small 8mer peptide is somewhat expected.

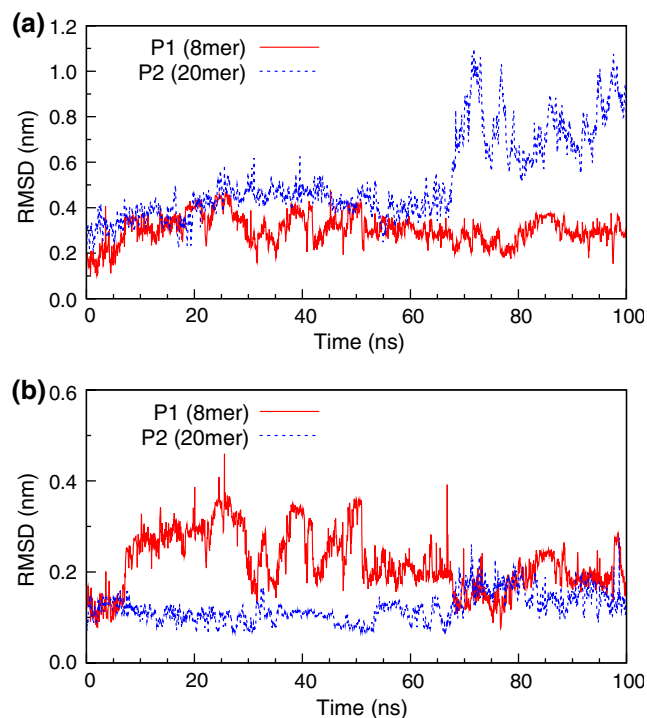


Fig. 3 **a** Root mean square displacement (RMSD) of the backbone atoms during MD trajectories: P1 for the 8mer peptide, P2 for the 20mer peptide. **b** RMSD time evolution considering only the backbone atoms of the 314–319 fragment of P1 and P2

What is worthy to note is that the same sequence retains considerably its starting conformation when embedded in a bigger peptide sequence. From this point of view, one can say that the conformation of the P2 peptide is closer to the initial structure, regarding the N-terminal sequence, thus this corresponding to the P1 peptide. This implies that shortening a peptide sequence affects drastically the conformation, and the peptide loses even the small stability that might possess. From conformational point of view the two peptides are not equivalent. However, different conformational stability does not necessarily imply loss of activity. It is known for example the P1 (8mer) peptide retains most of the biological activity (Biris et al. 2003a). These data indicate that a receptor can bind a small peptide regardless of its relatively unordered structure, and that well-defined peptide conformations are not absolute prerequisites for biological activity.

Backbone Conformation and Secondary Structure Analysis

The original strand conformation of 8mer peptide (P1) was lost during equilibration period. Two dominant conformational clusters were observed during P1 trajectory. In a significant part of the trajectory frames (27.9%) all residues were found in coil conformation, without any particular preference for secondary structure stabilization. In the most dominant cluster (39.5% of the trajectory frames, 23.7% of TTTTTT and 15.8% of CTTTTC STRIDE assignment) a β -turn (type IV) was observed in the central part of the peptide. Other small fragments of the P1 peptide showed turn-like conformations for smaller parts of the trajectory. Interestingly, $i \leftarrow i + 3$ main chain hydrogen bonds that could stabilize β -turns were not observed. In all of the cases turn structure that were observed was of type IV.

In the P2 trajectory, as it listed in Table 1, it is evident that the original strand conformation of the 313–320 fragment was much better conserved than in the P1 case. Moreover, the existence of coil conformation in this fragment was found significantly reduced in comparison to the previously analyzed P1 case. On the other hand, 6mer clusters in the P2 case were less populated. The most populated clusters were in CCCCCC and CEETTT states with 16.8 and 16.7% of the trajectory frames, respectively. The fragment Glu₃₁₅Ser₃₁₆ in particular, was found in strand conformation in many other clusters that were appeared in shorter time during the MD trajectory. From this analysis it is evident the 6mer fragment 314–319 of the P2 peptide remained in a strand conformation, similar to the original conformation for significant amount of the time. The peptide has not showed a compact structure, and its flexibility was also confirmed RMSD analysis. However, it showed

Table 1 Conformational clusters of the 314–319 fragment of the P1 (8mer) and P2 (20mer) trajectories

	P1 (8mer)			P2 (20mer)		
	#	Secondary structure	% Occurrence	#	Secondary structure	% Occurrence
Conformational states were characterized as Coil (C), strand (E) or Turn (T) with the STRIDE program	1	CCCCCC	27.9	1	CCCCCC	16.8
	2	TTTTTT	23.7	2	CEETTT	16.7
	3	CTTTTC	15.8	3	TEETTT	9.6
	4	CCTTTT	11.0	4	CCTTTT	8.8
	5	TTTCCC	7.7	5	CCCTTT	6.4
	6	TTTTCC	7.3	6	CCCCCT	4.7
	7	TTTTTC	5.1	7	BEETTT	3.4

Table 2 Occurrence of β -turns within P1 (8mer) and P2 (20mer) peptide sequences, as calculated from the corresponding MD trajectories. Percentage of frames that met the geometrical criteria is given

Fragment	P1 (8mer)	P2 (20mer)
Y ₃₁₃ MES ₃₁₆	33.8	10.7
M ₃₁₄ ESR ₃₁₇	15.3	4.1
E ₃₁₅ SRA ₃₁₈	22.4	
S ₃₁₆ RAD ₃₁₉	37.3	22.9
R ₃₁₇ ADR ₃₂₀	14.1	37.7
A ₃₁₈ DRK ₃₂₁		9.6
D ₃₁₉ RKL ₃₂₂		8.1
K ₃₂₁ LAE ₃₂₄		6.1
L ₃₂₂ AEV ₃₂₅		5.5
A ₃₂₃ EVG ₃₂₆		12.2
E ₃₂₄ VGR ₃₂₇		10.1
G ₃₂₆ RVY ₃₂₉		10.3
V ₃₂₈ YLF ₃₃₁		25.2
Y ₃₂₉ LFL ₃₃₂		10.4

elements of ordered secondary structure not observed in the P1 case. The diversity and the plethora of the observed conformational transitions allow us to speculate that the time scale of the simulation was big enough to obtain a satisfactory level of sampling different conformations. This is also in agreement with the previously analyzed convergence of the simulations.

Several β -turns were found to exist, although their stability was quite marginal or moderate. Table 2 lists the β -turn assignments in the two trajectories. In the P1 trajectory the main β -turn found was in the E₃₁₅SRA₃₁₈ fragment (33.8%), while in the P2 trajectory, the main β -turn found was in the R₃₁₇ADR₃₂₀ fragment (37.7%). The later is in agreement when the β -turn observed in the crystal structure. Thus, the lower backbone RMSD values observed in the P2 trajectory, relatively to P1, considering only the 8mer peptide, can be ascribed to the existence of R₃₁₇ADR₃₂₀ the β -turn. It is worth to note that the E₃₁₅SRA₃₁₈ turn was not found during the P2 trajectory. As it also indicated by the Table 1, the N-terminal part of the

P2 peptide (that corresponds to the P1 sequence) was dominated by coil conformation.

Backbone Conformation of the 314–319 Fragment

Conformation of selected frames from the P1 and P2 trajectories are in shown in Fig. 4. It is evident that both peptides visited quite divergent conformational spaces. This is also true if we look at the Ramachandran maps of backbone dihedrals. Figure 5 shows the ϕ/ψ backbone dihedral angle distribution obtained from the two MD trajectories. As it can be seen, simulation of P1 (8mer) peptide resulted in ϕ/ψ combinations that scattered in considerable bigger areas than in P2 (20mer) simulation. This fact also corroborates the previous findings about the increased flexibility of the P1 peptide relatively to P2 peptide, and it is in accordance with the secondary structure analysis.

In order to address the relative coverage of the conformational space in P1 and P2 trajectories, the Fig. 6 was prepared. Plotting of entropy S after appending one trajectory to the other clearly indicates that the P2 trajectory covered less conformational space than the P1. Moreover, that conformations sampled during P2 trajectory were within sampled during P1 trajectory, thus the two trajectories overlap but the P1 trajectory contained the backbone conformations of the P2 trajectory. The estimated difference conformational entropy between the backbone atoms of 314–319 fragments was found $87 \text{ J}^{-1} \text{ K}^{-1} \text{ mol}^{-1}$ (as indicated by the arrow at the middle of the graph).

Salt Bridges and Hydrogen Bonding

Despite the presence of numerous charged groups in the P1 peptide sequence, the conformation of the peptide was not found to be stabilized by salt bridges. The relative stability of the hairpin structure in the P2 case is also evident from hydrogen bond analysis (Table 3). A main chain Arg₃₁₇ \leftarrow Arg₃₂₀ hydrogen bond was observed for 30.1% of the simulation time and provided moderate stabilization

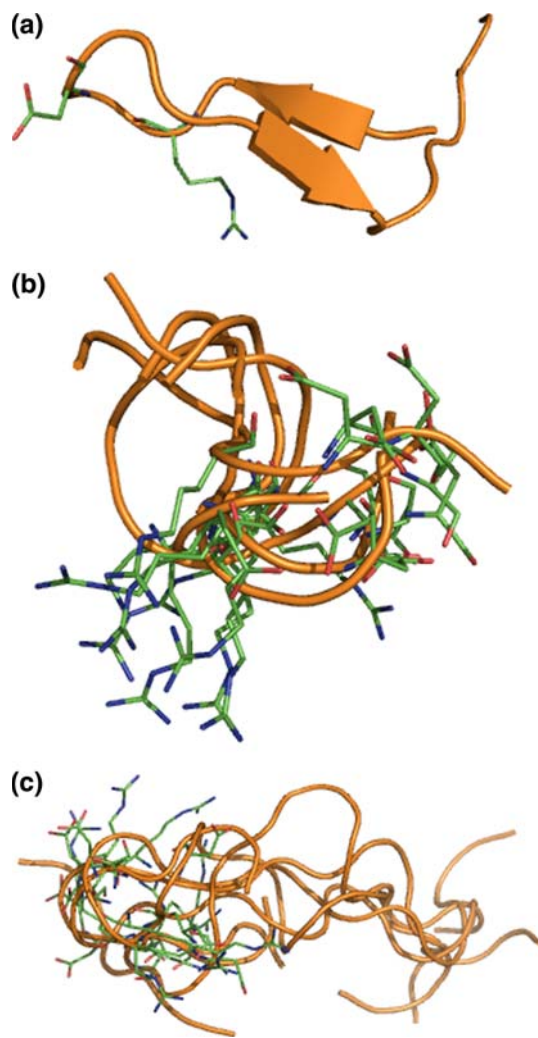


Fig. 4 **a** The P2 (20mer) peptide from the crystal structure, **b** five representative frames (every 20 ns) from the P1 trajectory and **c** five representative frames (every 20 ns) from the P2 trajectory. Backbone conformation is shown with *orange cartoons* while side chains of Arg₃₁₇ and Asp₃₁₉ residues are shown with *sticks*. (Color figure online)

of the β -turn around the Ala₃₁₈Asp₃₁₉ fragment. Tyr₃₁₃ \leftarrow Val₃₂₅, Met₃₁₄ \leftarrow Leu₃₂₂ and Glu₃₁₅ \leftarrow Leu₃₂₂ main chain hydrogen bonds also contributed to the hairpin's stability as they were observed for 15.3, 36.9 and 37.4% of the trajectory frames, respectively.

Overall, the electrostatic interactions did not play critical role in the stability of both peptides. This is somewhat unexpected, considering the abundance of the charged groups in the sequence of the peptides, which they also possessed uncapped N- and C-terminals. The absence of ordered structure in the case of P1 and the limited presence of secondary structural elements of P2 case indicate that electrostatic interactions in aqueous solution cannot dominate peptide's stability, at least in the current case.

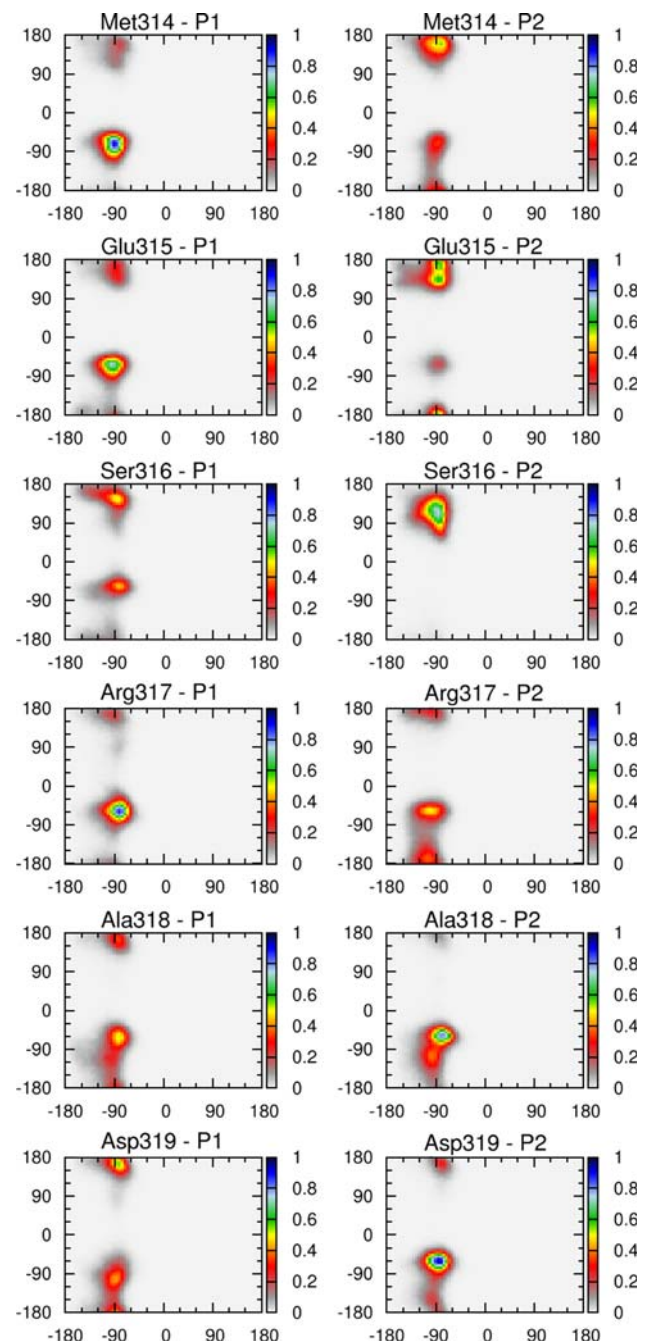


Fig. 5 Distribution of ϕ/ψ backbone dihedral angles of selected residues (314–319). Two dimension probability density plots were obtained, with ϕ angle in the horizontal axis and ψ in the vertical one. The adjacent *colour bar* at each graph is used to identify regions of low (*blue*) versus high (*red*) populations (percent of frames in 5° dihedral angle bin search). (Color figure online)

Biological Implications of the RAD Fragment Conformation

It has been hypothesized (Stanica et al 2008; Stavrakoudis et al. 2001) that the RAD fragment of the octapeptide, which is homologous of the well known RGD sequence,

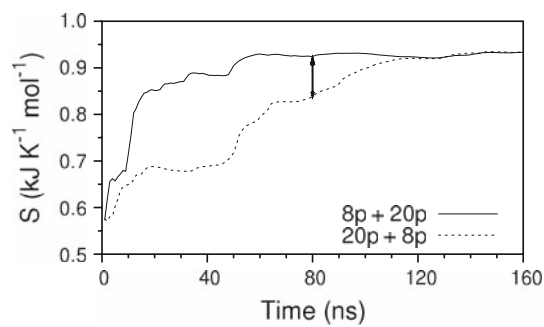


Fig. 6 Plot of estimated entropies of backbone atoms of the 314-319 fragment of the P1 and P2 peptides. Frames from the P1 were appended to the P2 trajectory and vice-versa. Last 80 ns from the two trajectories were used, assuming equilibrium was reached. See “Methods” for details of calculation. Arrow at 80ns indicates the entropy difference in conformational entropy of the backbone atoms

Table 3 Hydrogen interactions found in the P2 (20mer) peptide trajectory

Donor	Acceptor	% Occurrence
Tyr ₃₁₃ :N	Glu ₃₂₄ :O ^{ε1,2}	14.7
Met ₃₁₄ :N	Leu ₃₂₂ :O	36.9
Glu ₃₁₅ :N	Leu ₃₂₂ :O	5.2
Glu ₃₁₅ :N	Ala ₃₂₃ :O	
Arg ₃₁₇ :N	Glu ₃₁₅ :O	20.5
Arg ₃₁₇ :N	Arg ₃₂₀ :O	17.3
Arg ₃₁₇ :N ^ε	Glu ₃₁₅ :O ^{ε1,2}	35.4
Arg ₃₁₇ :N ^{η2}	Glu ₃₁₅ :O ^{ε1,2}	43.0
Leu ₃₂₂ :N	Glu ₃₁₅ :O	37.4
Val ₃₂₅ :N	Tyr ₃₁₃ :O	15.3
Arg ₃₂₇ :N ^ε	Glu ₃₂₄ :O ^{ε1,2}	24.6
Arg ₃₁₇ :N ^{η1,2}	Glu ₃₂₄ :O ^{ε1,2}	29.0

plays a significant role in the biological activity of the Y₃₁₃MESRADR₃₂₀. The side chain orientation of the arginine and aspartic residues has been classified as an important factor to inhibitory activity of such peptide analogues (Kostidis et al 2004; Stavarakoudis and Tsikaris 2008; Stavarakoudis et al. 2000). As a consequence, a dihedral angle of orientation (*pdo*) has been introduced, in order to account this particular conformational feature. The four atoms that constitute this dihedral angle are Arg:_iC^ζ, Arg:_iC^α, Asp_{i+2}:C^α and Asp_{i+2}:C^γ atoms, where *i* = 317 in one case for example (Arg₃₁₇-Asp₃₁₉). As it shown in Fig. 7, the P2 peptide preferred *pdo* values around -30° for the Arg₃₁₇-Ala-Asp₃₁₉ fragment. At the same time, this *pdo* angle showed wider distribution in the P1 peptide, with values closer to -90° . This is somewhat expected, if we take into consideration the previously discussed unordered structure of the P1 peptide. Similar preference, although

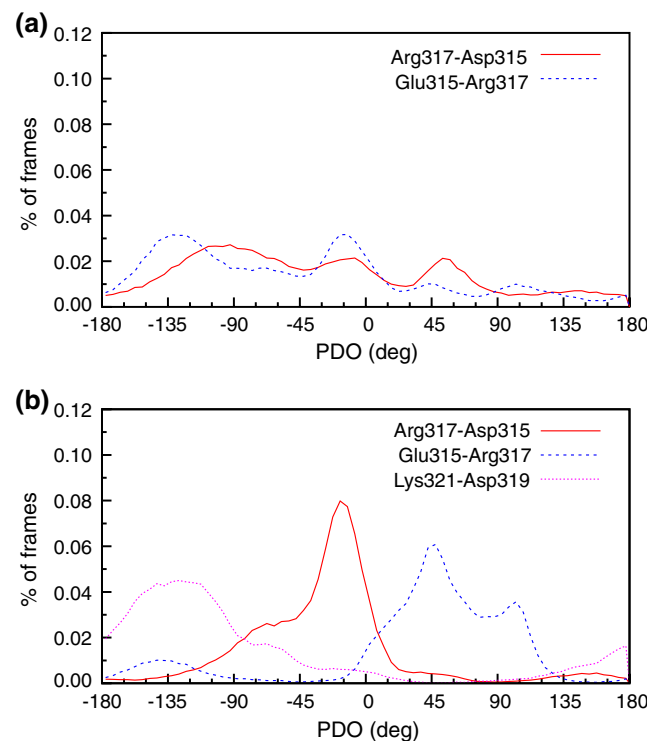


Fig. 7 Probability distribution of the pdo dihedral angle of orientation of the Arg/Lys and Asp side chains in **a** P and **b** P2 trajectories, respectively. Probabilities were calculated within 5° angle bin

with opposite signs ($\sim 90^\circ$) has been observed in Ac-RCDC-NH₂ peptide (Stavarakoudis and Tsikaris 2008). The corresponding value of *pdo* in the X-ray structure (starting conformation) was found 11.6° . Analysis of the NMR obtained bundle of structures of Ac-RGD-NH₂ peptide in DMSO solution (Biris et al 2003b) revealed that *pdo* dihedral angle averaged at -54.7° (17.6°) and ranged between -15.4° and 70.9° . These facts indicate that experimental results obtained from NMR or X-ray experiments and simulation results presented in this work advocate in a relative synplanar orientation of polar side chains of arginine and aspartic acid residues in RXD sequence. Proximity of these opposite charged groups is somewhat expected, although distances between Arg:C^ζ and Asp:C^γ atoms were found above 0.6 nm (can be 1.5 nm in some cases) indicating side chains can maintain synplanar orientation despite the weak nature of electrostatic interactions between them. Recent experimental and theoretical studies of model RGD peptides in gas phase also provided evidence for the synplanar orientation of Arg and Asp side chains (Li et al 2009; Gregoire et al 2007).

Both P1 and P2 peptides exhibited similar biological activity (Biris et al 2003b), despite the substantial differences in their conformation. This fact implies that the relatively high backbone flexibility of the P1 (8mer) peptide did not result in significant loss of activity.

Conclusions

The peptide fragments derived from the α_{IIb} sequence have studied with molecular dynamics simulations and their conformation has been analyzed. Sequences of 313–320 (P1) and 313–332 (P2) of the α_{IIb} protein, component of the integrin receptor, have been identified using epitope mapping techniques of overlapping peptides, to play important role in fibrinogen binding and platelet aggregation. The current study presented conformational analysis of these peptides in aqueous solution, by utilizing computer modeling and molecular dynamics simulations.

Both peptides showed considerable conformational flexibility. The P2 (20mer) analogue retained partly its initial strand conformation but the P1 analogue lost completely its initial conformation during MD trajectory. Despite this flexibility P1 did not lost its biological activity. As it has been hypothesized elsewhere (Mitsios et al. 2006; Papamichael et al. 2009; Stanica et al. 2008; Stavrakoudis et al. 2000), peptide with 313–320 sequence retained the ability to inhibit the platelet aggregation and fibrinogen binding, through the presence and side chain specific orientation of the RAD residues. The current study provides evidence of this synplanar orientation of Arg/Asp side chains, commonly found in both P1 and P2 analogues, despite the differences in backbone conformational status. The results are in line with previously reported analyses of NMR and X-ray data on similar sequences. This study provides also evidence that biologically active peptides, does not always have a well defined structure.

Acknowledgments Parallel execution of NAMD has been performed at the Research Center for Scientific Simulations (RCSS) of the University of Ioannina. The worldwide Open Source Community is gratefully acknowledged for releasing to the public domain all the computational tools (LINUX, NAMD, GNU, etc.) needed for this research work.

References

- Barth E, Kuczera K, Leimkuhler B, Skeel RD (1995) Algorithms for constrained molecular dynamics. *J Comput Chem* 16:1192–1209
- Berman HM, Westbrook J, Feng Z, Gilliland G, Bhat TN, Weissig H, Shindyalov IN, Bourne PE (2000) The protein data bank. *Nucleic Acids Res* 28:235–242
- Biris N, Abatzis M, Mitsios JV, Sakarellos-Daitsiotis M, Sakarellos C, Tsoukatos D, Tselepis AD, Michalis L, Sideris D, Konidou G, Soteriadou K, Tsikaris V (2003a) Mapping the binding domains of the alpha(IIb) subunit. A study performed on the activated form of the platelet integrin alpha(IIb)beta(3). *Eur J Biochem* 270:3760–3767
- Biris N, Stavrakoudis A, Politou AS, Mikros E, Sakarellos-Daitsiotis M, Sakarellos C, Tsikaris V (2003b) The Ac-RGD-NH2 peptide as a probe of slow conformational exchange of short linear peptides in DMSO. *Biopolymers* 69:72–86
- Craig D, Gao M, Schulten K, Vogel V (2004) Structural insights into how the MIDAS ion stabilizes integrin binding to an RGD peptide under force. *Structure* 12:2049–2058
- Darden T, York D, Pedersen L (1993) Particle mesh Ewald: an $N \log(N)$ method for Ewald sums in large systems. *J Chem Phys* 98:10089–10092
- Delano W (2002) The PYMOL molecular graphics system. Delano Scientific, San Carlos
- Döker R, Maurer T, Kremer W, Neidig K, Kalbitzer HR (1999) Determination of mean and standard deviation of dihedral angles. *Biochem Biophys Res Commun* 257:348–350
- Duan Y, Kollman PA (1998) Pathways to a protein folding intermediate observed in a 1-microsecond simulation in aqueous solution. *Science* 282:740–744
- Espinoza-Fonseca LM (2009) Leucine-rich hydrophobic clusters promote folding of the N-terminus of the intrinsically disordered transactivation domain of p53. *FEBS Lett* 583:556–560
- Feller SE, Zhang YH, Pastor RW, Brooks BR (1995) Constant pressure molecular dynamics simulation: the Langevin Piston method. *J Chem Phys* 103:4613–4621
- Frishman D, Argos P (1995) Knowledge-based protein secondary structure assignment. *Proteins* 23:566–579
- Glykos NM (2006) Carma: a molecular dynamics analysis program. *J Comput Chem* 27:1765–1768
- Gregoire G, Gaigeot MP, Marinica DC, Lemaire J, Schermann JP, Desfrancois C (2007) Resonant infrared multiphoton dissociation spectroscopy of gas-phase protonated peptides. Experiments and Car-Parrinello dynamics at 300 K. *Phys Chem Chem Phys* 9:3082–3097
- Hansson T, Oostenbrink C, van Gunsteren WF (2002) Molecular dynamics simulations. *Curr Opin Struct Biol* 12:190–196
- Hsu STD, Peter C, Van Gunsteren WF, Bonvin MJJ (2005) Entropy calculation of HIV-1 Env gp120, its receptor CD4, and their complex: an analysis of configurational entropy changes upon complexation. *Biophys J* 88:15–24
- Humphrey W, Dalke A, Schulten K (1996) VMD: visual molecular dynamics. *J Mol Graph* 14:33–38
- Humphries MJ (2000) Integrin structure. *Biochem Soc Trans* 28:311–339
- Jorgensen WL, Chandrasekhar J, Madura JD, Impey RW, Klein ML (1983) Comparison of simple potential functions for simulating liquid water. *J Chem Phys* 79:926–935
- Karplus M, McCammon JA (2002) Molecular dynamics simulations of biomolecules. *Nat Struct Biol* 9:646–652
- Karplus M, Sali A (1995) Theoretical studies of protein folding and unfolding. *Curr Opin Struct Biol* 5:58–73
- Kostidis S, Stavrakoudis A, Biris N, Tsoukatos D, Sakarellos C, Tsikaris V (2004) The relative orientation of the Arg and Asp side chains defined by a pseudodihedral angle as a key criterion for evaluating the structure-activity relationship of RGD peptides. *J Pept Sci* 10:494–509.
- Li X, Wang H, Bowen KH, Gregoire G, Lecomte F, Schermann J-P, Desfrancois C (2009) The parent anion of the RGD tripeptide: photoelectron spectroscopy and quantum chemistry calculations. *J Chem Phys* 130:art. no. 214301
- Lorenzo B, Duccio F, Francesco P, Paolo De Ros R, Michel S, Ulf S (2007) A dynamical study of antibody-antigen encounter reactions. *Phys Biology* 4:172–180
- Mitsios JV, Tambaki AP, Abatzis M, Biris N, Sakarellos-Daitsiotis M, Sakarellos C, Soteriadou K, Goudevenos J, Elisaf M, Tsoukatos D, Tsikaris V, Tselepis AD (2004) Effect of synthetic peptides corresponding to residues 313–332 of the alphaIIb subunit on platelet activation and fibrinogen binding to alpha-IIbeta3. *Eur J Biochem* 271:855–862

- Mitsios JV, Stamos G, Rodis FI, Tsironis LD, Stanica MR, Sakarellos C, Tsoukatos D, Tsikaris V, Tselepis AD (2006) Investigation of the role of adjacent amino acids to the 313-320 sequence of the alphaIIb subunit on platelet activation and fibrinogen binding to alphaIIb beta3. *Platelets* 17:277–282
- Morikis D, Lambris JD (2004) Physical methods for structure, dynamics and binding in immunological research. *Trends Immunol* 25:700–707
- Morra G, Meli M, Colombo G (2008) Molecular dynamics simulations of proteins and peptides: from folding to drug design. *Curr Protein Pept Sci* 9:181–196
- Painter CA, Cruz A, Lopez GE, Stern LJ, Zavala-Ruiz Z (2008) Model for the peptide-free conformation of Class II MHC proteins. *PLoS Biol* 3:e2403
- Papamichael ND, Stathopoulou EM, Roussa VD, Tsironis LD, Kotsia AP, Stanica RM, Moussis V, Tsikaris V, Katsouras CS, Tselepis AD, Michalis LK (2009) Effect of a synthetic peptide corresponding to residues 313 to 320 of the alphaIIb subunit of the human platelet integrin alphaIIb beta3 on carotid artery thrombosis in rabbits. *J Pharmacol Exp Ther* 329:634–640
- Phillips DR, Charo IF, Parise LV, Fitzgerald LA (1988) The platelet membrane glycoprotein IIb-IIIa complex. *Blood* 71:831–843
- Phillips JC, Braun R, Wang W, Gumbart J, Tajkhorshid E, Villa E, Chipot C, Skeel RD, Kale L, Schulten K (2005) Scalable molecular dynamics with NAMD. *J Comput Chem* 26:1781–1802
- Salsmann A, Schaffner-Reckinger E, Kieffer N (2006) RGD, the Rho'd to cell spreading. *Eur J Cell Biol* 85:249–254
- Santiveri CM, Jimenez MA, Rico M, Van Gunsteren WF, Daura X (2004) Beta-hairpin folding and stability: molecular dynamics simulations of designed peptides in aqueous solution. *J Pept Sci* 10:546–565
- Schlitter J (1993) Estimation of absolute and relative entropies of macromolecules using the covariance-matrix. *Chem Phys Lett* 215:487–496
- Smith BJ, Daura X, Van Gunsteren WF (2002) Assessing equilibration and convergence in biomolecular simulations. *Proteins* 48:487–496
- Stanica MR, Benaki D, Rodis FI, Mikros E, Tsoukatos D, Tselepis A, Tsikaris V (2008) Structure-activity relationships of alphaIIb 313-320 derived peptide inhibitors of human platelet aggregation. *J Pept Sci* 14:1195–1202
- Stavarakoudis A (2009a) Computational modeling and molecular dynamics simulations of a cyclic peptide mimotope of the CD52 antigen complexed with CAMPATH-1H antibody. *Mol Simul*. doi:10.1080/08927020903124593
- Stavarakoudis A (2009b) A disulfide linked model of the complement protein C8γ complexed with C8α indel peptide. *J Mol Mod* 15:165–171
- Stavarakoudis A, Tsikaris V (2008) Computational studies on the backbone-dependent side chain orientation induced by the (S, S)-CXC motif. *J Pept Sci* 14:1259–1270
- Stavarakoudis A, Bizos G, Eleftheriadis D, Kouki A, Panou-Pomonis E, Sakarellos-Daitsiotis M, Sakarellos C, Tsoukatos D, Tsikaris V (2000) A three-residue cyclic scaffold of non-RGD containing peptide analogues as platelet aggregation inhibitors: design, synthesis, and structure-function relationships. *Biopolymers* 56:20–26
- Stavarakoudis A, Bizos G, Eleftheriadis D, Kouki A, Panou-Pomonis E, Sakarellos-Daitsiotis M, Sakarellos C, Tsoukatos D, Tsikaris V (2001) A three-residue cyclic scaffold of non-RGD containing peptide analogues as platelet aggregation inhibitors: design, synthesis, and structure-function relationships. *Biopolymers* 56:20–26
- Stavarakoudis A, Demetropoulos IN, Sakarellos C, Sakarellos-Daitsiotis M, Tsikaris V (1997) Design, synthesis and catalytic activity of a serine protease synthetic model. *Int J Pept Res Ther* 4:481–487
- Stavarakoudis A, Makropoulou S, Tsikaris V, Sakarellos-Daitsiotis M, Sakarellos C, Demetropoulos IN (2003) Computational screening of branched cyclic peptide motifs as potential enzyme mimetics. *J Pept Sci* 9:145–155
- Stavarakoudis A, Tsoulos IG, Shenkarev ZO, Ovchinnikova TV (2009) Molecular dynamics simulation of antimicrobial peptide arenicin-2: beta-hairpin stabilization by noncovalent interactions. *Biopolymers* 92:143–155
- Takada Y, Ye X, Simon S (2007) The integrins. *Genome Biol* 8:215
- Tatsis VA, Stavarakoudis A, Demetropoulos IN (2008) Molecular Dynamics as a pattern recognition tool: an automated process detects peptides that preserve the 3D arrangement of Trypsin's Active Site. *Biophys Chem* 133:36–44
- Tatsis VA, Stavarakoudis A, Demetropoulos IN (2006) Lysinebased-TrypsinActSite (LysTAS): a configurational tool of the TINKER software to evaluate Lysine based branched cyclic peptides as potential chymotrypsin-mimetics. *Mol Simul* 32:643–644
- Tatsis V, Tsoulos IG, Krinas CS, Alexopoulos C, Stavarakoudis A (2009) Insights into the structure of the PmrD protein with molecular dynamics simulations *Int J Biol Macromol* 44:393–399
- Toukmaji AY, Board JA (1996) Ewald summation techniques in perspective: a survey. *Comput Phys Comm* 95:73–92
- Tsoulos IG, Stavarakoudis A (2009) eucb: a C++ program for trajectory analysis. <http://stavarakoudis.econ.uoi.gr/eucb>
- van Gunsteren WF, Berendsen HJC (1990) Computer simulation of molecular dynamics: methodology, applications, and perspectives in chemistry. *Agnew Chem Int Ed Engl* 29:992–1023
- van Gunsteren WF, Dolenc J, Mark AE (2008) Molecular simulation as an aid to experimentalists. *Curr Opin Struct Biol* 18:149–153
- Voordijk S, Hansson T, Hilvert D, van Gunsteren WF (2000) Molecular dynamics simulations highlight mobile regions in proteins: a novel suggestion for converting a murine V(H) domain into a more tractable species. *J Mol Biol* 300:963–973
- Wan S, Coveney P, Flower DR (2004) Large-scale molecular dynamics simulations of HLA-A*0201 complexed with a tumor-specific antigenic peptide: can the alpha3 and beta2m domains be neglected? *J Comput Chem* 25:1803–1813
- Wang H, Sung SS (1999) Effects of turn residues on beta-hairpin folding—a molecular dynamics study. *Biopolymers* 50:763–976
- Xiao T, Takagi J, Collier BS, Wang JH, Springer TA (2004) Structural basis for allostery in integrins and binding to fibrinogen-mimetic therapeutics. *Nature* 432:59–67
- Xiong JP, Stehle T, Zhang R, Joachimiak A, Frech M, Goodman SL, Arnaout MA (2002) Crystal structure of the extracellular segment of integrin alpha Vbeta3 in complex with an Arg-Gly-Asp ligand. *Science* 296:151–155
- Yaneva R, Springer S, Zacharias M (2009) Flexibility of the MHC class II peptide binding cleft in the bound, partially filled, and empty states: a molecular dynamics simulation study. *Biopolymers* 91:14–27
- Yoda T, Sugita Y, Okamoto Y (2007) Cooperative folding mechanism of a beta-hairpin peptide studied by a multiconformational replica-exchange molecular dynamics simulation. *Proteins* 66:846–859
- Zacharias M, Springer S (2004) Conformational flexibility of the MHC class I alpha1-alpha2 domain in peptide bound and free states: a molecular dynamics simulation study. *Biophys J* 87:2203–2214